European Journal of Pharmaceutics and Biopharmaceutics 78 (2011) 49–57

Contents lists available at ScienceDirect

European Journal of Pharmaceutics and Biopharmaceutics

journal homepage: www.elsevier.com/locate/ejpb

Research paper

Zero-order release of 5-fluorouracil from PCL-based films featuring trilayered structures for stent application

Lei Lei [a], Xi Liu [a], Yuan-Yuan Shen [a], Jie-Ying Liu [b], Mu-Fei Tang [a], Zhong-Min Wang [c,d,*], Sheng-Rong Guo [a,*], Liang Cheng [a]

[a] School of Pharmacy, Shanghai Jiao Tong University, Shanghai, China
[b] School of Medicine, Shanghai Jiao Tong University, Shanghai, China
[c] School of Radiation Medicine and Public Health, Suzhou University, Suzhou, China
[d] Department of X-ray, Shanghai Jiao Tong University, Shanghai, China

ARTICLE INFO

Article history:
Received 30 March 2010
Accepted in revised form 11 January 2011
Available online 19 January 2011

Keywords:
Film
Poly(ε-caprolactone) (PCL)
5-Fluorouracil (5-FU)
Controlled drug delivery
Scanning electron microscopy (SEM)

ABSTRACT

A trilayered Poly(ε-caprolactone) (PCL)-based film with a coating layer (CL), a drug-storing layer (DSL) loaded with antitumor drug 5-Fluorouracil (5-FU) and a backing layer (BL) are presented for film-based stent application in malignant stricture or stenosis. V-C diffusion cells were used to investigate the drug permeability of the CL, while scanning electron microscopy (SEM) was employed for observing the microscopic architectures and morphologies. Drug release from the trilayered films exhibited a zero-order pattern, and the release process followed an 'outer-to-inner' pattern. The formation mechanism and influencing factors of the zero-order drug release pattern were in-depth elucidated, and factors affecting the drug release were also investigated. The reduction of initial drug loading in DSL slowed the drug release and diminished the zero-order release pattern. Drug permeability of the CL depended significantly on CL thickness, but not significantly on PCL molecular weight. Besides, the addition of PEG porogen in the CL accelerated the drug release by elevation of the drug permeability of CL, and the action mechanism of PEG was revealed by the PEG release test and SEM. The loading of 5-FU in the CL could lead to a two-phased release profile. This study revealed the potential of the trilayered film in controlled drug delivery to intraluminal tumor due to its highly tunable zero-order drug release.

1. Introduction

Tumors in physiological tubular structures, such as vessels, esophagus, bile duct, prostate, and urethral duct, usually lead to the local occlusion or stenosis [1]. In these cases, the stent, a tubular medical device, is used to keep the patency of strictured or occluded physiological tubular structure and maintain their normal physiological functions. However, in-stent stenosis and restenosis due to the overgrowth of tumor tissue occur frequently in practical applications. With the advantage of simultaneously providing mechanical support and releasing antitumor agents to actively treat local intraluminal tumor, drug-eluting stents (DES) revolutionized the treatment of malignant body conduit or tubular structure diseases and have moved into the limelight.

To prepare DES, various drug loading strategies have been reported, including incorporating drugs in the holes or cavities of the metal stent struts [2] and loading drug in the polymeric coatings or membranes wrapped around the bare metallic stent [3]. Polymeric drug-loaded coating has been adopted in most metallic DES by virtue of its ability of providing sustained drug release. However, non-biodegradable polymers, which are widely used for stent coating, have been found to be partly responsible for late adverse events and pathologic reactions, including hypersensitivity [4]. What's more, when metallic stents' treatment period or life span expires, they need to be removed by a second surgery which may inflict extra pain on patients. Hereby, fully biodegradable DES based on biocompatible polymers could be more advantageous and preferable [5]. So far, a wide variety of biodegradable DES have been investigated and clinically tested [6], and the results are encouraging [5]. Most DES are based on fibers [1,7] or films [8–11], and the drugs are incorporated in the stent coating or in the stent strut bulk. Among these reported DES, however, few can achieve zero-order drug release (ZODR) kinetics.

The drug release pattern is critical to the treatment performance of a drug delivery system. For effective treatment, drug doses must fit with a specific window whose lower limit is above the therapeutic threshold and whose upper limit is below the toxic level [12]. However, most of the current drug delivery devices

Abbreviations: 5-FU, 5-fluorouracil; BL, backing layer; CL, coating layer; DES, drug-eluting stent; DSL, drug-storing layer; PCL, poly(ε-caprolactone); PEG, polyethylene glycol; SEM, scanning electron microscopy; ZODR, zero-order drug release.

* Corresponding authors. School of Pharmacy, Shanghai Jiao Tong University, 800 Dongchuan Road, Shanghai 200240, China. Tel./fax: +86 21 34204793.
E-mail address: srguo@sjtu.edu.cn (S.-R. Guo).

0939-6411/$ - see front matter © 2011 Elsevier B.V. All rights reserved.
doi:10.1016/j.ejpb.2011.01.003

release drug in typical "fast-then-slow" drug release manners, and consequently, a stable drug concentration level cannot be provided. Thus, a drug delivery system which can produce a ZODR kinetics is desirable for the maintenance of tissue drug concentration at a stable level [13]. In intraluminal tumor treatment by DES, a ZODR pattern is of essential importance, because it can help maintain tumor tissue drug concentration at a stable, effective level for a long time, which is very favorable for killing tumor cells.

In the present study, a series of trilayered films were designed to produce a ZODR pattern in DES application. Poly(ε-caprolactone) (PCL) was selected as the film matrix due to its good biocompatibility, drug permeability, biodegradability (with a relatively slow degradation rate) and anti-fatigue capability [12,14,15], while 5-fluorouracil (5-FU) was applied as the model drug because of its wide use in the treatment of a range of cancers [16,17]. The films have a sandwich-shaped structure, that is, a drug-storing layer (DSL), loaded with 5-FU, is sandwiched between a coating layer (CL) and a backing layer (BL). The adjustable ZODR pattern of this trilayered film was demonstrated by the *in vitro* drug release results which showed time-independent release kinetics. Furthermore, the formation mechanism of the ZODR pattern was revealed through *in vitro* drug release tests and V-C diffusion tests. The dependences of drug release kinetics on the drug loading in the DSL, the thickness and PCL molecular weight of the CL, and the PEG contents in the CL are presented as well. Based on the SEM observations combined with the release results, the structural evolution, drug release process and action mechanism of PEG porogen were discussed.

2. Materials and methods

2.1. Materials

5-FU was purchased from Nantong Jinghua Pharmaceutical Co., Ltd. (Nantong, China) and micronized by a planetary ball-mill (Pulverisette 6, Fritsch, Germany). The sizes of the 5-FU particles were measured, by a laser particle sizer (Analysette 22 Compact, Fritsch, Germany), to be in a range of 8–40 μm. Polyethylene glycol (PEG 20,000) was purchased from Sinopharm Chemical Reagent Co., Ltd. (Shanghai, China). PCL 50 K (M_w = 50,000) was from Daicel Polymer Ltd. (Minatoku, Tokyo, Japan), while PCL 80 K (M_w = 80,000) was from Shenzhen Bright-China Industrial Co., Ltd. (Shenzhen, China). HPLC grade methanol was obtained from Shanghai Xingke Biochemistry CO., Ltd. All other chemicals were of analytical grade and used as received. Deionized water was used when preparing the mobile phase, buffers and drug donor solutions.

2.2. Film preparation

The single layers consisting of the trilayered film were prepared as follows: first, various combinations of ingredients (i.e., PCL, 5-FU particles and PEG) were fed into the chamber of a HAAKE Rheocord System (Rheocord 90, HAAKE Mess-Technic GmbH, Germany) and mixed thoroughly at 80 °C and a rotor speed of 45 rpm for 30 min; then, the resulting blends were hot-pressed into films with predetermined thickness on a compression molding machine (XLB-D, Shanghai No. 1 Rubber Machine Factory) at 100 °C, followed by cooling to room temperature.

To prepare trilayered film, the three single layers (CL, DSL and BL) consisting of a trilayered film were agglutinated together layer by layer with toluene as the agglutinant and then pressed under the pressure of 0.25 kg/cm^2 for 5 min to form a robust trilayered structure. The resulting trilayered film was left in a vacuum oven at 35 °C for 3 d to remove the residual toluene.

2.3. X-ray diffraction analysis (XRD)

XRD analyses of the single layers with various compositions, 5-FU crystals and PEG powders were performed using an X-ray diffractometer (D/max 2200, Rigaku, Japan) equipped with Cu Kα radiation source (40 kV, 20 mA). The XRD traces were recorded over a 2θ range of 5–45° at a rate of 5°/min.

2.4. HPLC

5-FU concentration was determined using an HPLC system (LC-10Advp, SHIMAZU, Japan), equipped with a UV–Vis detector (SPD-10Avp, SHIMAZU, Japan) and a Diamonsil C18 reversed phase column (particle size 5 μm, 4.6 × 250 mm). The UV detection was performed at 266 nm with the column temperature maintained at 35 °C. The mobile phase was water (0.3% HAc)-methanol (94:6, v/v), and the flow rate was 1 mL/min. The linear range of drug concentration was 0.1–60 μg/mL with a relevant coefficient of 0.9999. The sample solution was filtered through a 0.45 μm filter membrane before injection. The injection volume was 50 μL, and the retention time for 5-FU was 5.6 min. 5-FU concentration was calculated according to a calibration curve plotted by using different concentrations of 5-FU in PBS.

2.5. Drug permeation

2.5.1. Franz cells diffusion

Unilateral drug release from the DSL or through the drug-free BL of a trilayered film was determined using Franz cells with a diffusion area of 3.15 cm^2. The trilayered film was mounted on the Franz cells with the test side in contact with 6.5 mL of PBS pH 7.4 in the receiver compartment and the other side facing the empty donor compartment. The temperature of PBS in receiver compartment was maintained at 37 °C using a water bath and stirred constantly with a magnetic stir bar at a rate of 250 rpm. At predetermined time points, medium in the receiver chamber was completely withdrawn for HPLC determination and replaced with 6.5 mL of fresh PBS.

2.5.2. Horizontal cells diffusion

The tested single CL was mounted between the donor and receiver chambers of a set of horizontal, water-jacketed, side-bi-side V-C cells (Shanghai Kaikai Scientific Technology, Shanghai, China) with an effective diffusion area of 0.78 cm^2. This set of cells has a similar setup as the well known PermeGear Side-Bi-Side Cells (PA, USA). The donor chamber was filled with 5 mL of saturated 5-FU solution (about 16 mg/mL) in PBS pH 7.4, while the receiver chamber was filled with 5 mL of blank PBS. Both solutions in the donor and receiver chambers were maintained at 37 °C and constantly stirred with magnetic stir bars at a rate of 250 rpm to minimize the boundary effect. At predetermined time points, the solution in the receiver chamber was completely withdrawn for HPLC determination and replaced with 5 mL fresh PBS.

2.6. In vitro release

The trilayered/bilayered film was cut into discs (diameter 1.2 cm), and then the circumference side of the disc was sealed with PCL 80 K at a thickness of about 200 μm to prevent the direct contact of the DSL with the release media. Each disc was placed in a polyethylene tube containing 15 mL of PBS. The tube was placed in a shaking water bath at 37 °C with a shaking speed of 65 rpm. At predetermined time points (i.e., at increasing intervals of hours and days), the release medium was completely withdrawn and replaced with 15 mL of fresh PBS to maintain sink conditions. The 5-FU concentration in the release medium was assessed by HPLC. The fractional drug release was calculated by normalizing the sum of

released mass of 5-FU by the original mass of 5-FU in film before release. Each experiment was performed in quadruplicate.

2.7. PEG release

The PEG concentration (or the amount of PEG released into the release medium) was determined by a colorimetric method based on the formation of a colored complex between two hydroxyl groups of PEG, Ba^{2+} and an iodine molecule (I_2) [18]. In this study, deionized water rather than PBS was used as the release medium for PEG release, because the phosphate radical in PBS could interfere with the color reaction. An aliquot of 4 mL of properly diluted release medium was mixed with 1 mL of 5% (w/v) $BaCl_2$ solution in deionized water. To this mixture, 1 mL of solution prepared by dissolving 1.3 g I_2, and 3.5 g KI in 100 mL of deionized water was added. Color was allowed to develop for 5 min at room temperature, and absorbance was read using a spectrophotometer at 565 nm against a reagent blank prepared in the same way. The PEG concentration was calculated using a calibration curve realized by using different concentrations of PEG in deionized water in the same conditions.

2.8. Scanning electron microscopy (SEM)

The surface and cross-section morphologies of the films were observed using a JSM-7401F scanning electron microscope (SEM) (JEOL, Tokyo, Japan). The cross-section of film was obtained by freeze fracturing the film in liquid nitrogen. Prior to imaging, samples were mounted vertically on a metal sample holder and sputter coated with gold–palladium at a thickness of 7.5 nm (Emitech K-575 Sputter Coater). SEM images were obtained at 1 kV accelerating voltage and 20 mA current.

3. Results and discussion

3.1. Characterization of the trilayered PCL stent films

3.1.1. Structure and characteristics of the trilayered PCL stent films

As illustrated in Fig. 1, the trilayered film was comprised of three layers, i.e. a coating layer (CL), a drug-storing layer (DSL) and a backing layer (BL). The compositions of all trilayered stent films are listed in Table 1. According to the in vivo application concept, the designed trilayered film can be further fabricated into tubular polymeric stent (Fig. 1). Here, the BL facing the lumen was used to block the undesirable drug release towards the lumen of physiological tube and to offer supporting mechanical strength, while the CL touching the tissue wall was applied to achieve a ZODR. With regard to the DSL, it acted as a drug reservoir, and in this layer, drug loading of up to 60% was achieved. Besides, in some of the trilayered films, hydrophilic PEG was added in the CL as porogen to regulate the drug release.

3.1.2. XRD analysis of the layers with various compositions

The physical states of the components in the single layers consisting of the trilayered films were examined by the analysis of the XRD traces of 5-FU crude powder, PEG powder as well as the drug- and/or PEG-incorporated single-layer films. As shown in Fig. 2, the 5-FU crude powder exhibited high crystallinity as characterized by an intense diffraction peak at 29° and a series of weak peaks at 2θ of 16°, 21° and 32°, which were consistent with those reported by other literatures [19,20]; while the neat PCL film displayed two characteristic peaks at 21° and 24° [21]. The diffractograms for 5-FU-loaded layers showed obvious crystalline peaks at the same 2θ angles as in the diffractograms for the 5-FU crude powder and neat PCL film. These results manifest that the encapsulated 5-FU in the films was in its crystalline state, namely the 5-FU crude particles were not dissolved but existed at concentrations far higher than its saturated level in the PCL film matrix. In addition, the PEG in the CL layer containing 15% PEG was also in its crystalline state, as proved by the weak peak appeared at 19° in the XRD diffractogram (Fig. 2).

3.2. In vitro drug release

3.2.1. Unidirectional drug release pattern

As mentioned above, the BL of the trilayered film was applied to block the undesirable drug release towards the lumen of the physiological tubular structure and to offer supporting mechanical

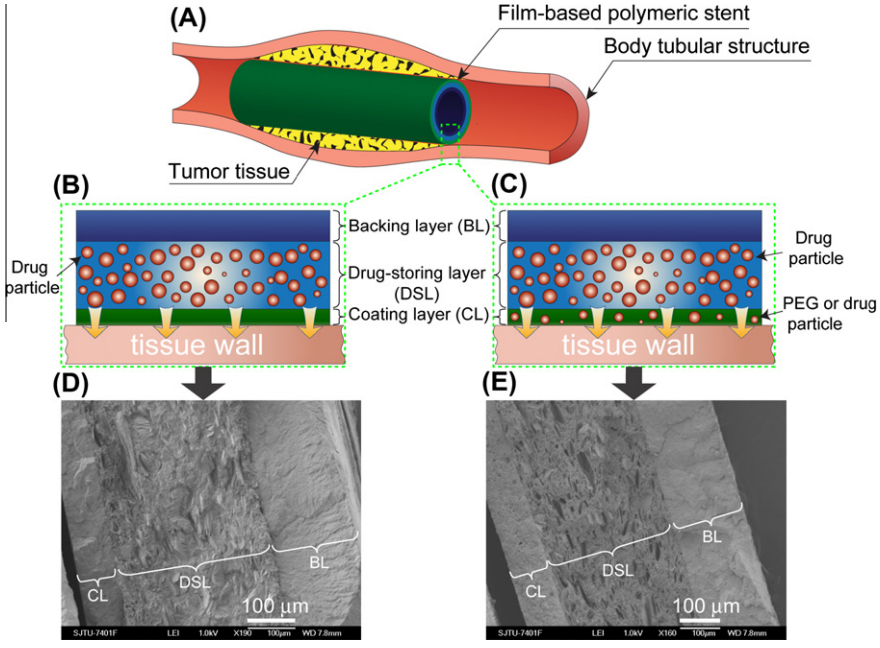

Fig. 1. Schematic diagrams of the in situ application mode (A), cross-section structures and drug release patterns of the trilayered films (B–E). The coating layer (CL) can be composed of PCL alone (B) or loaded with PEG or drug (C). The SEM images clearly show the trilayered cross-sections of the films with their CL consisting of PCL alone (D) and containing 15% PEG (E), respectively, after incubation for 106 d in PBS. (For interpretation of the references to colour in this figure legend, the reader is referred to the web version of this article.)

Table 1
Compositions of all trilayered stent films.

Film	Number of layers	Total thickness (μm)	Coating layer (CL) (thickness, 100 μm)			Drug-storing layer (DSL) (thickness, 350 μm)		Backing layer (BL) (thickness, 200 μm)
			Drug (%)	PCL 50 K (%)	PEG (%)	PCL 50 K (%)	Drug (%)	PCL 80 K (%)
Film 1	3	650	–	100	–	40	60	100
Film 2	3	650	–	95	5	40	60	100
Film 3	3	650	–	85	15	40	60	100
Film 4	3	650	–	85	15	60	40	100
Film 5	3	650	20	80	–	40	60	100
Film 6	2	550	–	–	–	40	60	100

strength. Thus, it was necessary to investigate its performance in blocking drug release. Franz cells were used to investigate the drug releases from the two sides (the DSL and the BL) of Films 1 and 3, which had different CLs but the same BL, and the drug release profiles are shown in Fig. 3. In general, both the drug releases from the CLs and that from the BL underwent a rate-constant pattern. During the investigation period, more than 2–50 times larger amounts (206 μg/cm^2 for Film 1 and 4896 μg/cm^2 for Film 3) of 5-FU were released from the CL side, while a smaller amount (101 μg/cm^2) from the BL. This means that the majority (nearly 70–98%) of the drug in the DSL was released from the CL, while much less drug was released from the BL, which in turn demonstrated the contribution of the BL in achieving unidirectional drug release pattern.

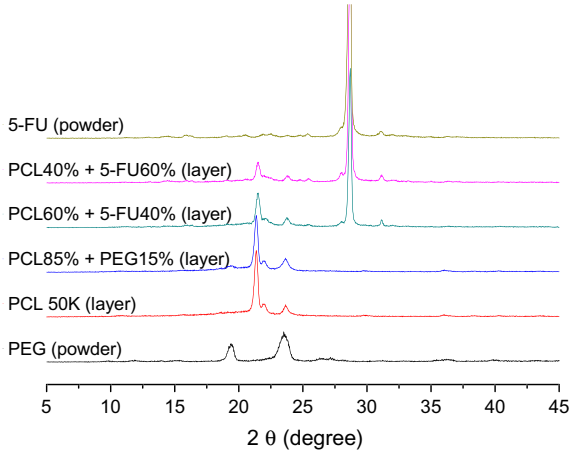

Fig. 2. XRD traces for the tested single-layer films as well as the crude 5-FU and PEG powders. The results indicate that the incorporated 5-FU and PEG were in their crystalline states. (For interpretation of the references to colour in this figure legend, the reader is referred to the web version of this article.)

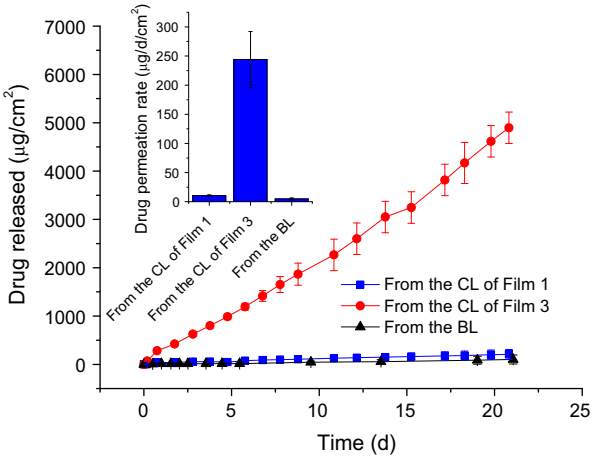

Fig. 3. Cumulative drug release profiles of 5-FU from the different CLs and the same BL of films 1, 2 and 3 (mean ± SD, $n = 3$). Franz cells were used to investigate the drug release from a single side. (For interpretation of the references to colour in this figure legend, the reader is referred to the web version of this article.)

3.2.2. Zero-order drug release behavior of the trilayered films

In our trilayered film, the CL was applied to control the drug release, specifically to produce a ZODR pattern. Here, it should be noted that Film 6 was considered as part of Films 1, 2 and 3, because bilayered Film 6 (without a CL) had the identical DSL and BL as trilayered Films 1, 2 and 3. By the comparison of the release

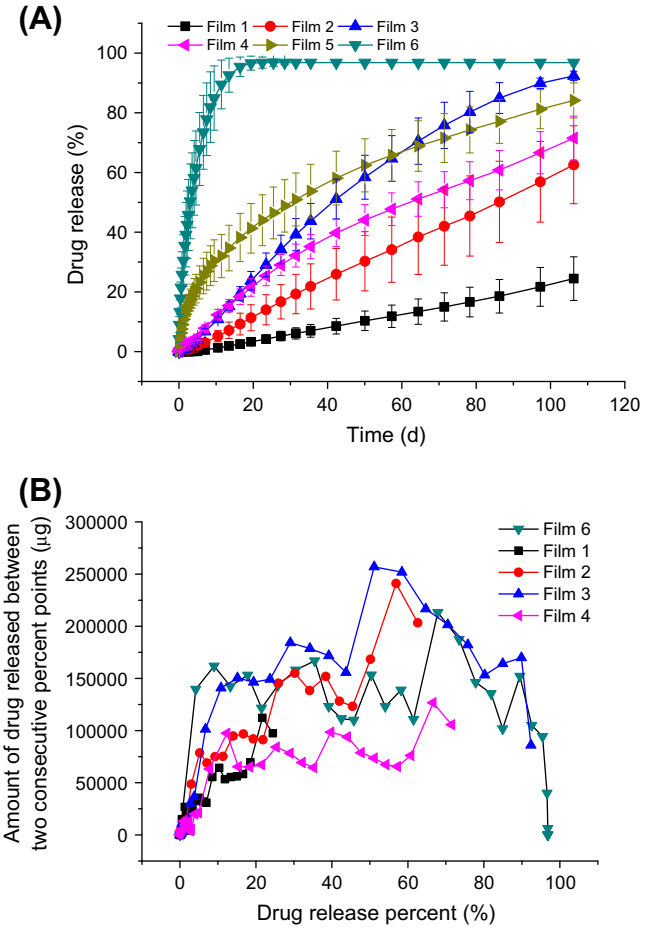

Fig. 4. (A) Drug release profiles of the trilayered films versus bilayered films (without a CL) (mean ± SD, $n = 4$). (B) Drug release amount as a function of drug release percent. The trilayered films had a variety of drug release profiles. (For interpretation of the references to colour in this figure legend, the reader is referred to the web version of this article.)

Table 2
Fitting results of the drug release data by zero-order and Higuchi models.

Film	Time period (day)	Higuchi model ($M_t/M_\infty = kt^{0.5}$)[a]		Zero-order model ($M_t/M_\infty = kt$)[a]	
		k	r	k	r
Film 1	0–106	–	–	0.2302	0.9996
Film 2	0–106	–	–	0.5879	0.9993
Film 3	0–106	0.0802	0.9571	0.9838	0.9889
Film 4	0–106	0.0612	0.9752	0.7081	0.9851
Film 5	0–35	9.1322	0.9987	–	–
	40–106	–	–	0.4005	0.9966
Film 6	0–18	0.2765	0.9918	–	–

[a] M_t/M_∞, fractional drug release; t, the release time; k, a constant of the drug/polymer system; r, correlation coefficient.

profiles of Films 6 and other trilayered films (Fig. 4), it can be found that after the introduction of a CL, the drug release duration was noticeably extended and the drug release was effectively lowered and stabilized. The good fitting results of the release data of the trilayered films by the zero-order model [22], with the correlation coefficient above 0.999 (Table 2), demonstrated that the drug release was in a zero-order manner. In addition, GPC results showed that the PCL molecular weights in the films just decreased by about

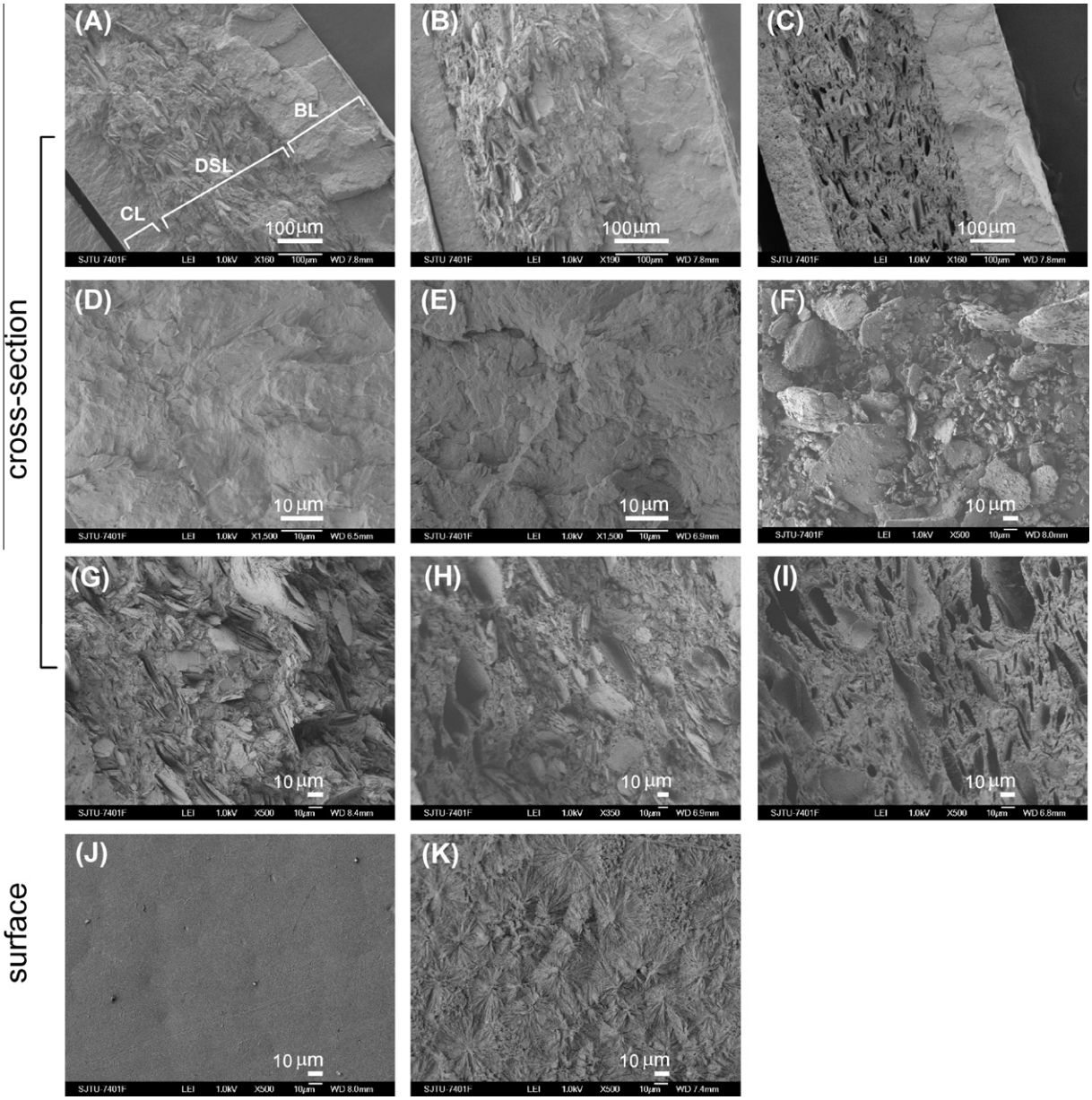

Fig. 5. Evolution of surface and cross-section morphologies with drug release: (A) Film 2 before release; (B) Film 2 at 106 d; (C) Film 3 at 106 d. (D) $CL_{Film\ 1}$ before release; (E) $CL_{Film\ 1}$ at 106 d; (F) 5-FU particles; (G) $DSL_{Film\ 2}$ before release; (H) $DSL_{Film\ 2}$ at 106 d; (I) $DSL_{Film\ 3}$ at 106 d; (J) $CL_{Film\ 1}$ before release; (K) $CL_{Film\ 1}$ at 106 h.

3–5% after the release test (data not shown), indicating no significant PCL degradation and erosion of matrix. Accordingly, the CL, DSL and BL of the trilayered films were substantially stable during the drug release, and the drug release was dominated by a diffusion mechanism.

It is apparent in Fig. 4A that drug release from bilayered Film 6 (without a CL) was much faster than the other trilayered films with an additional CL (Films 1, 2, and 3), which indicates that the CL effectively controlled the drug release from the trilayered films. For Films 1 and 2 with the CLs containing no PEG and lower content of PEG (5%), respectively, the drug release curves were highly linear, showing that they underwent ZODR behavior during the investigation period. Compared with Film 2, Film 3 (with the same DSL as Film 2, but a different CL containing 15% PEG) underwent an inferior zero-order drug release and exhibited a slowly decreasing release rate before 60% of the drug was released.

To elucidate the mechanism and influencing factors for the achievement of ZODR, we plotted the drug release amounts as a function of the drug release percent (Fig. 4B). As shown in Fig. 4B, the curves for Films 1 and 2 are essentially under that for Film 6, which means that during the same drug release-percent interval investigated, Film 6 released more drug than Films 1 and 2. This also indicates that during the investigation periods, drug releases from Films 1 and 2 (i.e., from their DSL, through the CL, to the PBS, as illustrated by Fig. 1) were limited by their CLs, which led to a ZODR pattern. As a contrast, the plotted curve for Film 3 is not continuously under that for Film 6 (Fig. 4B). This manifests that before 25% of the drug was released, Film 6 released more drug than Film 3 (with an additional CL over Film 6). This also suggests that during this stage, drug release from the DSL of Film 3 through the CL to the PBS medium was limited by its CL. During the later stage (after 65% of the drug was released), however, Films 6 and 3 released very close amounts of drug in highly similar manners (Fig. 4B). This implies that at the later stage, the CL of Film 3 was no longer the limit step of drug release from the DSL through the CL to the PBS, while drug release from the DSL turned to be the limit step, which in turn explains the high similarity of the time-dependent drug release profiles of Films 3 and 6 which having the same DSL during their last release periods (see Fig. 4B).

These results testify that the application of a CL could achieve a ZODR pattern. It is reasonable to draw the conclusion that the realization of a good ZODR pattern was dependent on whether the CL could exert its drug release-limiting function. Accordingly, it was suggested that to obtain a ZODR pattern, the drug release from the DSL should be always faster than the drug permeation through the CL to ensure the release-limiting function of the CL. Many factors (e.g. drug loading in the DSL, composition of the CL and drug loading in the CL) can be utilized to adjust the drug release profile and rate, and this will be discussed in the later sections.

3.3. Structural evolution of the films and drug release process

On the whole, all the investigated films underwent similar structural evolution with drug release. As can be seen in Fig. 5A, the cross-section of the trilayered film displayed clearly three layers (i.e. the CL, DSL and BL) (Fig. 5A). The surfaces of the CL and the BL were smooth and flat before the drug release (Fig. 5J), and the cross-sections of the CL and BL of the films were dense and devoid of pores before drug release test (Fig. 5A and D). As a contrast, the cross-section of the DSL was homogeneously dispersed with many granular and lamellar crystals (Fig. 5A and G). These crystals had the same shapes and size as the 5-FU crude particles shown in Fig. 5F. Based on this as well as the fore-mentioned XRD results, the crystals embedded in the PCL matrix can be identified as the incorporated 5-FU particles. However, after the 106-d drug release, it was noteworthy that there existed three distinct layers with two clear boundaries (Fig. 5C) and that many discrete micro-cavities could be observed in the DSL (Fig. 5I), and the size and shape of these micro-cavities were nearly identical to that of 5-FU particles (Fig. 5F), suggesting that these pores were the voids left by the released 5-FU particles. Comparing Fig. 5D and E, it can be found that, unlike the DSL, the cross-section of BL did not undergo any

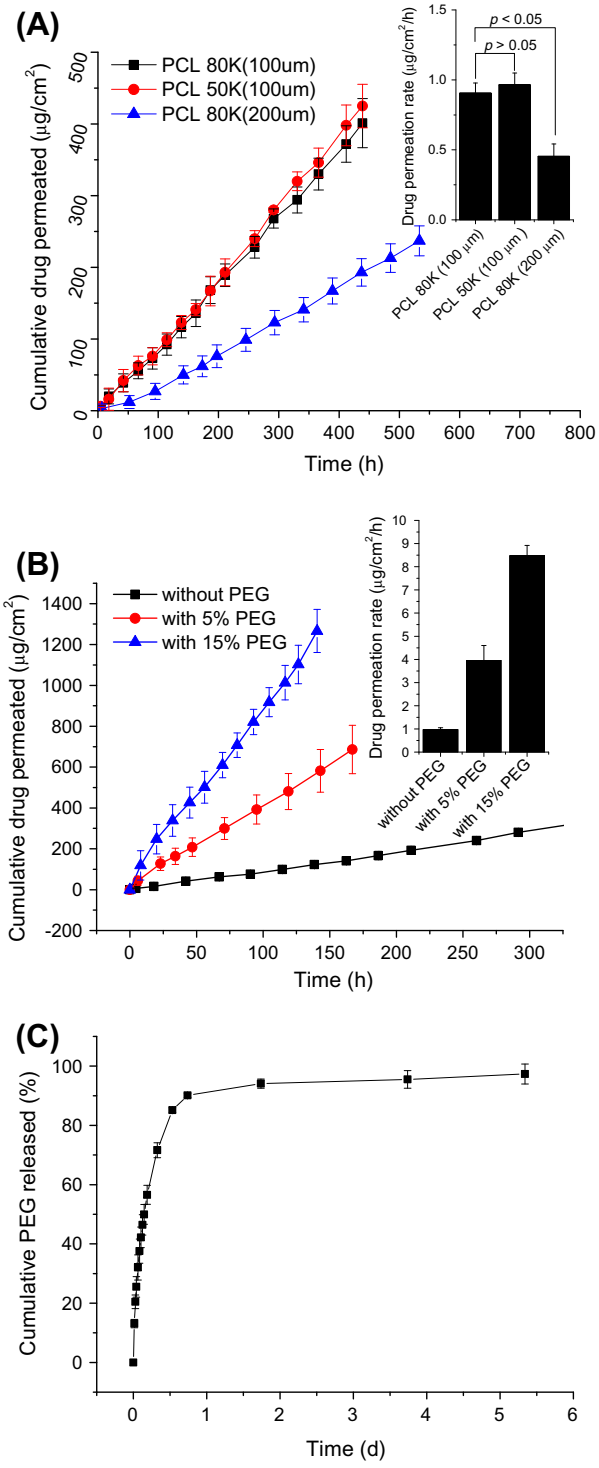

Fig. 6. Dependence of drug permeation rate on PCL molecular weight and layer thickness of CL (A), as well as the additive PEG content (B). (C) Profile for PEG release from the CL of Film 3 containing 15% PEG. (For interpretation of the references to colour in this figure legend, the reader is referred to the web version of this article.)

apparent change. However, the surface of CL or BL became rough after drug release (Fig. 5K), which is attributed to the slight superficial erosion of PCL.

From Fig. 5A–C, it can be observed that after 106-d drug release, some micro-cavities appeared on the CL side (left) of the DSL of Film 2, while the other part of the cross-section was compact. Additionally, considering the fact that at 106 d just 65% drug loaded in Film 2 was released (Fig. 4A), it can be predicted that when the drug is entirely released, the cross-section of the DSL would be as porous as the that for Film 3 (which had the same DSL with Film 2 and released substantially all of the drug at 106 d). This indicated that the majority of drug was released from the CL side of the trilayered film and also that the drug release followed a pattern of gradual direction of from outer to inner (namely, an 'outer-to-inner' pattern) with the drug release boundary shifting from outer side to inner side. This release pattern was also observed in the other PCL-based preparations [12,21].

3.4. Impact of drug loading in DSL on the drug release

Comparing the drug release curves of Films 3 and 4 (Fig. 4A), it was found that although they had the same CL and BL, Film 3 (with a higher drug loading of 60% in the DSL) showed a steeper release curve than Film 4 (with a lower drug loading of 40%). Besides, according to the fitting results listed in Table 2, the obtained k value for Film 4 (0.9838) was larger than that for Film 3 (0.7081). These results show that the trilayered film with higher drug loading (Film 3) could release drug faster than that with lower drug loading (Film 4). Observing Fig. 5H and I, it can be found that the number of micro-cavities, left behind by the released 5-FU particle, was also correlated with the initial drug loading in DSL. Film with higher drug loading generated a larger number of micro-cavities at the same release time, which in turn accelerated the subsequent later drug release. When the CL was not the rate-limiting step of the drug release, like in the cases of Films 3 and 4, the drug loading in the DSL could influence the drug release. On one hand, a higher drug loading indicates a lower PCL content in the DSL, weakening the retarding effect of PCL matrix and thus facilitating the drug release; on the other hand, the larger amount of micro-cavities formed by the film with higher drug loading can accelerate its subsequent later drug release.

3.5. Effect of PCL molecular weight and thickness of CL on drug permeability

V-C diffusion cells were used to investigate the drug permeability of CL with different thicknesses and PCL molecular weights. As shown in Fig. 6A, the cumulative amount of drug permeated through the CL from the saturated 5-FU PBS solution increased linearly with time. The slopes, as depicted in columns in Fig. 6A, of the lines indicate the drug permeation rates. Comparing the permeation rates, it can be found that the molecular weight of PCL in the CL had no significant ($p > 0.05$) influence on the drug permeation rate of the CL with a thickness of 100 μm, which may be attributed to the close values of the two molecular weights used, 50,000 and 80,000. As a contrast, the CL thickness exerted significant ($p < 0.05$) influence on the drug permeation rate. The CL with a larger thickness had lower drug permeation rate.

3.6. Impact of PEG addition into the CL on the drug release

Comparing the drug release curves of Films 1, 2 and 3 with different PEG contents (Fig. 4A), it is clear that the drug release rate increased with the PEG content in the CL of the trilayered film. To further verify the drug release-regulating ability of the CL, V-C diffusion cells were used to investigate the drug permeabilities of the single CLs containing 0%, 5% and 15% of PEG. Cumulative amounts of drug permeated through the CLs as a function of time showed straight lines (Fig. 6B), and the slopes of the lines increased with the PEG content. These results indicate that the addition of PEG effectively increased the drug permeability of the CL, thus accelerating the drug release from trilayered film.

To explore the action mechanism of PEG, SEM and examination of PEG release from the CL was carried out. As shown in Fig. 7A, with the addition of 5% PEG, the surface of the CL of Film 2 was still flat and smooth like the PEG-free CL of Film 1 (Fig. 5J), and the cross-section was essentially compact with a few pores (Fig. 7D). Notwithstanding, after 106-d *in vitro* release, the surface of Film

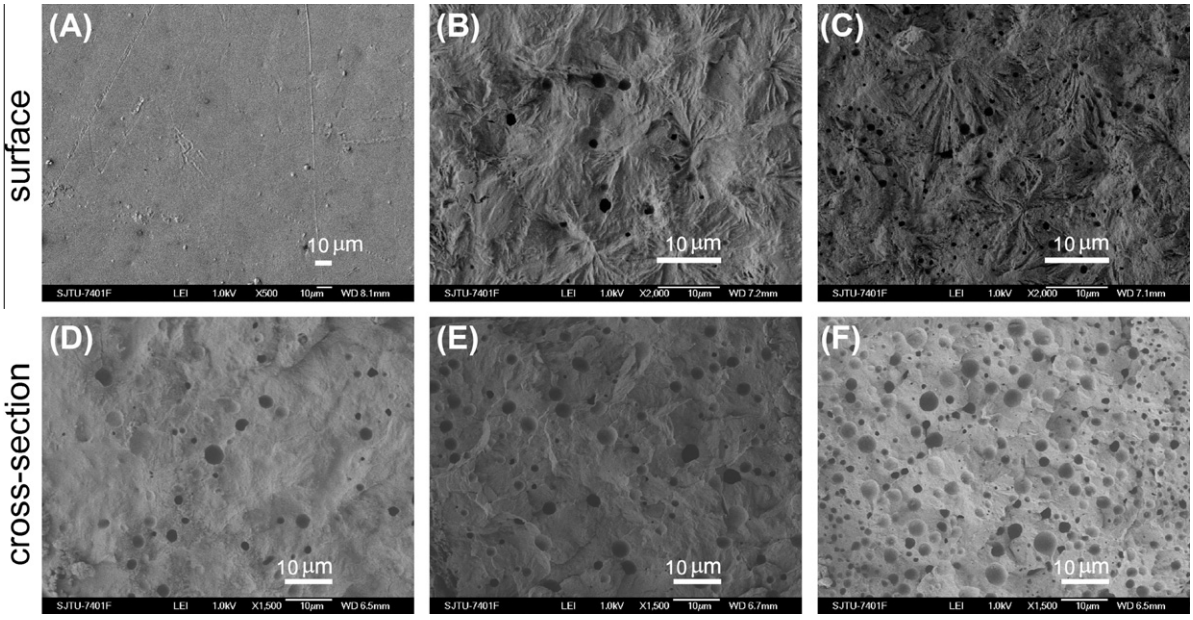

Fig. 7. The surface and cross-section morphologies of CLs containing various contents of PEG during 106-d drug release: (A and D) $CL_{Film\ 2}$ (5% PEG) before release; (B and E) $CL_{Film\ 2}$ (5% PEG) at 106 d; (C and F) $CL_{Film\ 3}$ (15% PEG) at 106 d.

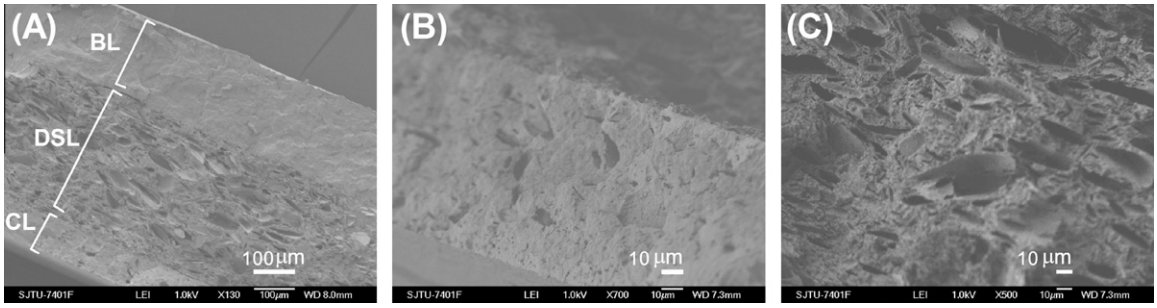

Fig. 8. Cross-section of Film 5 with the CL loaded with 20% 5-FU after 106-d release. The cross-section exhibits three layers (A), i.e., BL, porous CL (B) and porous DSL (C).

2 with 5% PEG (Fig. 7B) and Film 3 with 15% PEG (Fig. 7C) was rough and with many micro-pores, which are, respectively, due to the erosion of superficial PCL and release of PEG, respectively [23,24]. Also, many small micro-pores appeared on the cross-sections of Films 2 and 3 (Fig. 7E and F, respectively). It is noticeable that the number of micro-pores on the surface and cross-section of the CL increased with the PEG content. Hence, the enhancement of drug permeability by the PEG addition was probably ascribed to the formation of porous PCL matrix [24,25]. The PEG release curve presented in Fig. 6C shows that PEG incorporated in the CL of Film 3, which contained 15% PEG, was substantially released out within about 1 d. This suggests that the porous CL could form rapidly within a short time, compared with the several-month release duration, which enabled a steady zero-order release. These results manifest that the strategy of adding PEG porogen into the CL can effectively elevate the drug release rate by producing a porous CL, and the changing of PEG content can be utilized to regulate the drug release.

3.7. Two-phased drug release behavior due to the loading of drug in CL

As shown in Fig. 4A and Table 2, unlike Films 1, 2 or 3, the release of drug from Film 5 (with its CL loaded with 20% of 5-FU) followed a two-phased pattern, namely a first square-root-of-time-dependent (0–35 d, $r = 0.9987$) and then zero-order pattern (40–106 d, $r = 0.9966$). To probe the formation mechanism of the two-phased pattern, the cross-section structure was examined by SEM. SEM images show that the cross-section of Film 5, after 106-d release, exhibited clearly three layers (Fig. 8A), among which both the CL (Fig. 8B) and DSL (Fig. 8C) were full of micro-cavities, due to the release of incorporated 5-FU particles. Also, it is obvious that the porosity of CL (Fig. 8B) was much lower than DSL (Fig. 8C), indicating that drug permeation through the DSL could be much faster than that through the CL and that drug release from the DSL matrix should be limited by the CL. In addition, as discussed in Section 3.4, 5-FU release from the PCL matrix followed an 'outer-to-inner' pattern, indicating that the drug release from the CL of Film 5 occurred prior to that from the DSL. Based on the above analyses, it is concluded that the square-root-of-time-dependent drug release at the first stage was attributed to the initial release of drug from the CL matrix, while the ZODR behavior at later stage was contributed by the previously formed porous CL which controlled the subsequent drug release from the DSL.

4. Conclusion

We have produced trilayered films with the capability of releasing drug in a zero-order pattern. The ZODR behavior could be adjusted by changing the initial drug loading in the DSL, altering the initial PEG content in the CL or loading drug in the CL. The ZODR pattern of the trilayered film was determined by whether the CL can be continuously the limiting step of drug release. Accordingly, it was suggested that to obtain a ZODR pattern, the drug release from the DSL should be always faster than the drug permeation through the CL. Hereby, altering the compositions of the CL and DSL can be utilized to regulate the ZODR. On one hand, reducing drug loading in DSL could slower the drug release from the DSL and possibly deteriorate the ZODR pattern. On the other hand, the addition of PEG in CL could accelerate the drug release. The tuning mechanism of added PEG in the CL was its rapid release and consequent formation of porous CL with higher drug permeability. The loading of drug in the CL could be an alternative approach to obtain a two-phased drug release pattern which is composed of a first time-dependent phase and a later time-independent phase. By virtue of its highly tunable drug release, the trilayered films can be an attractive drug delivery system for intraluminal tumor treatment.

Acknowledgements

This work was supported by National Natural Science Foundation of China (NSFC) (30872554 and 81071244), Shanghai Science and Technology Committee (1052nm01000 and 10441902000), the National Comprehensive Technology Platforms for Innovative Drug R&D (2009ZX09301-007), and National Special Platform for New Drug R&D (2009ZX09301-007). The authors would like to thank Instrumental Analysis Center of Shanghai Jiao Tong University for their technical support.

References

[1] A. Kotsar, T. Isotalo, I. Uurto, J. Mikkonen, P. Martikainen, M. Talja, M. Kellomaki, J.P. Salenius, T.L.J. Tammela, Urethral in situ biocompatibility of new drug-eluting biodegradable stents: an experimental study in the rabbit, BJU Int. 103 (2009) 1132–1135.
[2] A. Finkelstein, D. McClean, S. Kar, K. Takizawa, K. Varghese, N. Baek, K. Park, M.C. Fishbein, R. Makkar, F. Litvack, N.L. Eigler, Local drug delivery via a coronary stent with programmable release pharmacokinetics, Circulation 107 (2003) 777–784.
[3] Q. Guo, S. Guo, Z. Wang, A type of esophageal stent coating composed of one 5-fluorouracil-containing EVA layer and one drug-free protective layer: in vitro release, permeation and mechanical properties, J. Control. Release 118 (2007) 318–324.
[4] J. Ako, H.N. Bonneau, Y. Honda, P.J. Fitzgerald, Design criteria for the ideal drug-eluting Stent, Am. J. Cardiol. 100 (2007) 3M–9M.
[5] T. Tsuji, H. Tamai, K. Igaki, E. Kyo, K. Kosuga, T. Hata, M. Okada, T. Nakamura, S. Fujita, S. Takeda, S. Motohara, H. Uehata, Biodegradable stents as a platform to drug loading, Int. J. Cardiovasc. Intervent. 5 (2003) 13–16.
[6] M. Zilberman, R.C. Eberhart, Drug-eluting bioresorbable stents for various applications, Annu. Rev. Biomed. Eng. 8 (2006) 153–180.
[7] M. Zilberman, K.D. Nelson, R.C. Eberhart, Mechanical properties and in vitro degradation of bioresorbable fibers and expandable fiber-based stents, J. Biomed. Mater. Res. Part B 74 (2005) 792–799.
[8] M. Zilberman, Y. Shifrovitch, M. Aviv, M. Hershkovitz, Structured drug-eluting bioresorbable films: microstructure and release profile, J. Biomater. Appl. 23 (2009) 385–406.
[9] M.C. Chen, C.T. Liu, H.W. Tsai, W.Y. Lai, Y. Chang, H.W. Sung, Mechanical properties, drug eluting characteristics and in vivo performance of a genipin-crosslinked chitosan polymeric stent, Biomaterials 30 (2009) 5560–5571.

[10] A. Mochizuki, T. Niikawa, I. Omura, S. Yamashita, Controlled release of argatroban from PLA film – effect of hydroxylesters as additives on enhancement of drug release, J. Appl. Polym. Sci. 108 (2008) 3353–3360.
[11] L.L. Lao, S.S. Venkatraman, Paclitaxel release from single and double-layered poly(DL-lactide-co-glycolide)/poly(L-lactide) film for biodegradable coronary stent application, J. Biomed. Mater. Res. Part A 87A (2008) 1–7.
[12] C. Li, L. Cheng, Y. Zhang, S. Guo, W. Wu, Effects of implant diameter, drug loading and end-capping on praziquantel release from PCL implants, Int. J. Pharm. 386 (2010) 23–29.
[13] J. Weidner, Drug delivery, Drug Discov. Today 7 (2002) 632.
[14] V.R. Sinha, K. Bansal, R. Kaushik, R. Kumria, A. Trehan, Poly-[epsilon]-caprolactone microspheres and nanospheres: an overview, Int. J. Pharm. 278 (2004) 1–23.
[15] S.R. Jameela, N. Suma, A. Jayakrishnan, Protein release from poly(ε-caprolactone) microspheres prepared by melt encapsulation and solvent evaporation techniques: a comparative study, J. Biomater. Sci. Polym. Ed. 8 (1997) 457–466.
[16] L. Ozel, M.S. Ozel, A.B. Toros, M. Kara, K.S. Ozkan, G. Tellioglu, O. Krand, M. Koyuturk, I. Berber, Effect of early preoperative 5-fluorouracil on the integrity of colonic anastomoses in rats, World J. Gastroenterol. 15 (2009) 4156–4162.
[17] C.M. Dolinsky, N.N. Mahmoud, R. Mick, W. Sun, R.W. Whittington, L.J. Solin, D.G. Haller, B.J. Giantonio, P.J. O'Dwyer, E.F. Rosato, R.D. Fry, J.M. Metz, Effect of time interval between surgery and preoperative chemoradiotherapy with 5-fluorouracil or 5-fluorouracil and oxaliplatin on outcomes in rectal cancer, J. Surg. Oncol. 96 (2007) 207–212.
[18] E. Leo, B. Ruozi, G. Tosi, M.A. Vandelli, PLA-microparticles formulated by means a thermoreversible gel able to modify protein encapsulation and release without being co-encapsulated, Int. J. Pharm. 323 (2006) 131–138.
[19] M. Sairam, V.R. Babu, B.V.K. Naidu, T.M. Aminabhavi, Encapsulation efficiency and controlled release characteristics of crosslinked polyacrylamide particles, Int. J. Pharm. 320 (2006) 131–136.
[20] K.S.V.K. Rao, I. Chung, K.M. Reddy, C.S. Ha, PMMA-based microgels for controlled release of an anticancer drug, J. Appl. Polym. Sci. 111 (2009) 845–853.
[21] L. Cheng, S.R. Guo, W.P. Wu, Characterization and in vitro release of praziquantel from poly(epsilon-caprolactone) implants, Int. J. Pharm. 377 (2009) 112–119.
[22] P. Costa, J. Manuel, S. Lobo, Modeling and comparison of dissolution profiles, Eur. J. Pharm. Sci. 13 (2001) 123–133.
[23] I.C. Liao, S. Chen, J.B. Liu, K.W. Leong, Sustained viral gene delivery through core–shell fibers, J. Control. Release 139 (2009) 48–55.
[24] C.H. Lu, W.J. Lin, Permeation of protein from porous poly(ε-caprolactone) films, J. Biomed. Mater. Res. 63 (2002) 220–225.
[25] D. Pankajakshan, L.P. Philipose, M. Palakkal, K. Krishnan, L.K. Krishnan, Development of a fibrin composite-coated poly(ϵ-caprolactone) scaffold for potential vascular tissue engineering applications, J. Biomed. Mater. Res. Part B 87B (2008) 570–579.